Proceedings of the 7th JFPS International
Symposium on Fluid Power, TOYAMA 2008
September 15-18, 2008

P1-26

ANALYSIS AND DESIGN OF CRYOGENIC BALL VALVE

Dong-Soo KIM*, Myoung-Sub KIM*

*Roll-to-Roll PEMS Team, Nano Mechanical Systems Research Division
Korea Institute of Machinery & Materials
171, Jang-Dong, Yuseong-Gu, Daejeon, Korea
(E-mail: joseph@kimm.re.kr)

ABSTRACT

Natural gas is being hailed as alternative energy sources for a petroleum, because it is almost no emissions of pollutants in the environment. Use of equipment for liquefied natural gas, along with increased demand for natural gas is also growing. Cryogenic ball valve is used to control the liquified natural gas which temperature is -196℃, supplied pressure is 168kg/cm^2. To acquire the safety along with durability of cryogenic ball valve, we should consider the structural mechanics such as stress, deformation and dynamic vibration characteristics and identify those important aspects in the stage of preliminary design engineering. For the cryogenic ball valve, the assurance of structural integrity and operability are essential to meet not only normal, abnormal loading conditions but also functionality during a seismic event. In this study, analytical approach and results using finite element analysis and computational method are herein presented to evaluate the aspects of structural integrity along with operability of cryogenic ball valve. Moreover, we have done the optimal design through special processing and heat treatment and so on. Finally, we designed the high pressure cryogenic ball valve that accomplishes zero leakage.

KEY WORDS

LNG, Cryogenic, Ball valve, Analysis, Design

NOMENCLATURE

D : Stiffness matrix
σ : Stress
ε : Strain vector
$\bar{\varepsilon}$: Supposition Strain vector
Γ : Boundary
ku : Elastomer stress vector
u_g : Displacement stress vector
t_b : Boundary stress vector
MPa : Young module coefficient
kg/cm^2 : Pressure
kg/mm^3 : Density
I/℃ : Thermal Expansion coefficient
W/mm℃ : Heat conduction

1. INTRODUCTION

The process of the formation of natural gas (NG) is similar to that of coal. NG can be produced from oil wells as assistant gas; however, most of it is produced as non-assistant gas. 80~85% of NG is methane (CH_4), whose low concentration of hazardous substances makes it a valuable energy resource. However, because NG is difficult to store in large quantities and mass transportation requires a pipeline, technology for NG liquefaction has been developed to solve these problems, enabling mass storage and transportation over long distances. The demand for facilities for the storage, transportation and control of liquefied natural gas

(LNG) is rapidly increasing in line with the rising demand for LNG [1-2].

Most of the high-pressure, cryogenic ball valves are of the side-entry type, the insulation of which has to be cut open to carry out repairs. Therefore, top-entry type cryogenic valves have been adopted recently [3].

Top-entry type, high-pressure, cryogenic ball valves are subject to safety verification to prevent the types of accidents that can be caused by earthquake, fire, or explosion. Their specifications regarding leakage, being very strict, are satisfied by only a few products in the world.

In this study, a numerical analysis is conducted for the structural safety and the distribution of thermal stress and deformation by thermal shock under high pressure and very low temperature conditions, in order to assess the safety and reliability of the ball valves for LNG to provide a basis for the design and manufacturing of products which are safe from leakage under conditions of extreme temperature variance.

Figure 1 Photo of the valves are installed on vessels

2. Finite Element Analysis (FEA) on Ball Valves

2.1. Theoretical Equation for Analysis

Eq. (1) is a finite element equation for 3-dimensional loads[4].

$$\frac{\partial\sigma_{xx}}{\partial x} + \frac{\partial\sigma_{xy}}{\partial y} + \frac{\partial\sigma_{xz}}{\partial\sigma z} = 0$$

$$\frac{\partial\sigma_{yx}}{\partial x} + \frac{\partial\sigma_{yy}}{\partial y} + \frac{\partial\sigma_{yz}}{\partial\sigma z} = 0$$

$$\frac{\partial\sigma_{zx}}{\partial x} + \frac{\partial\sigma_{zy}}{\partial y} + \frac{\partial\sigma_{zz}}{\partial\sigma z} = 0 \qquad (1)$$

In order to obtain a variational equation for the numerical analysis of the finite element method (FEM), eq. (1) can be transformed into eq. (2) in a weak form.

$$\int_{\Omega} \overline{u}^T \Delta\sigma d\Omega = 0 \qquad (2)$$

Using Green's Theorem, we obtain eq. (3), where $\overline{\varepsilon}$ is a virtual deformation vector and Γ is the boundary.

$$\int_{\Omega} \overline{\varepsilon}^T \sigma d\Omega - \int_{\Gamma} \overline{u}^T t d\Gamma = 0 \qquad (3)$$

In order to substitute the boundary condition, the stress vectors can be represented by eq. (4).

$$t = -k(u - u_g) + t_b \qquad (4)$$

Substituting eq. (4) into eq. (3), we obtain eq (5).

$$\int_{\Omega} \overline{\varepsilon}^T D\varepsilon d\Omega - \int_{\Gamma} \overline{u}^T ku d\Gamma = \int_{\Gamma} \overline{u}^T (ku_g + t_b) d\Gamma \qquad (5)$$

Eq. (6) is the finite element equation, and eq. (7) and (8) represent the stiffness matrix K and external force vector f, respectively.

$$Kd = f \qquad (6)$$

$$K = \sum_{i=1}^{e} \left(\int_{\Omega_e} B^T D B \, d\Omega_e + \int_{\partial\Omega_{e\cap\Gamma}} N^T K N \, d\Gamma \right) \qquad (7)$$

$$K = \sum_{i=1}^{e} \left(\int_{\Omega_{e\cap\Gamma}} N^T (t_b + ku_g) \, d\Gamma \right) \qquad (8)$$

2.2. Analyses of Thermal Stress and Resistance against Earthquake

Figure 2 shows the result of the finite element modeling of a 12-inch cryogenic ball valve using HYPERMESH, which is an exclusive item of software for finite element analysis, and ANSYS, which is a commercial FEA software for structural analysis and evaluation. In order to conduct the optimal simulation of a real 12-inch cryogenic ball valve with the FEA model, a tetrahedron solid element was used and the solid45, which is an element for isotropic materials. The solid elements have an average size of 9mm and comprise 609,706 elements and 135,396 nodes. The x, y, and z axes were defined to represent the lateral, longitudinal and vertical coordinates, respectively.

The material of the valve was stainless steel A351-CF3. One pipe joint was fixed and the other was assumed to be movable in the direction of flow. The internal pressure and temperature were assumed to be 1.68kg$_f$/mm^2 and -196℃, respectively. The external temperature was assumed to be 20℃. Figure 3 shows the result of the thermal analysis at the normal operating temperature, wherein the maximum stress of 23.9kg$_f$/mm^2 appears at the center of the ball.

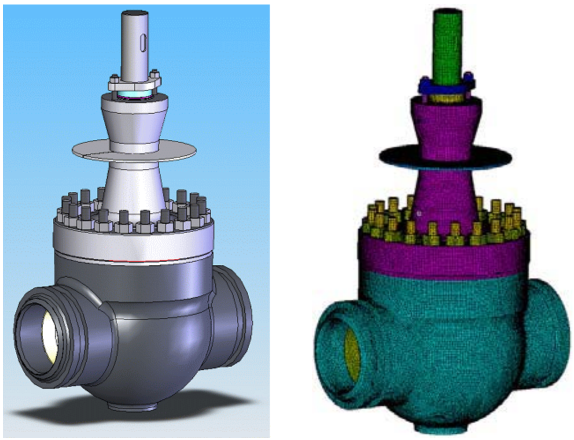

Figure 2 Result of the finite element modeling

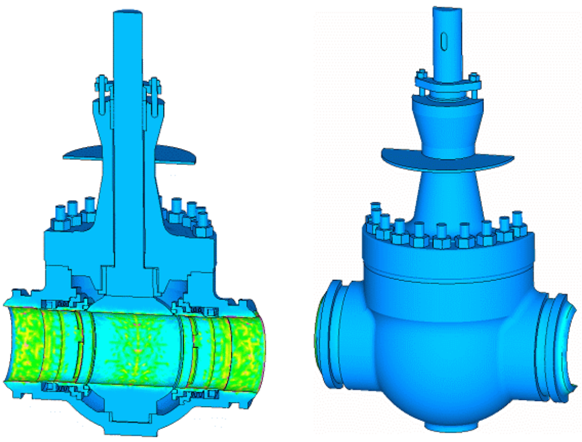

Figure 3 Result of the thermal analysis

2.3 . Earthquake-proof Analysis

The finite element modeling and its boundary conditions were conducted under the same conditions as those established for the thermal stress analysis, added with the conditions for earthquake-proof. The load conditions were classified into the empty weight of the device, internal pressure, temperature, Operating Basis Earthquake (OBE), and Safety Shutdown Earthquake (SSE). The OBE is an earthquake that does not force the LNG facility to stop operation, on the assumption that it will occur five times during the lifespan of the facilities. Therefore, the maximum stress exerted under an OBE is less than the elastic limit. The SSE, however, is a strong earthquake that may occur once throughout the lifespan of the facility. In this study, the device was applied with maximum acceleration in the x, y, and z directions, as presented in Table 1. The cases of the OBE and SSE include the earthquake accelerations in the vertical and horizontal directions, which are 2.0g, including the device weight, and 1.5g, in the vertical and x-y directions respectively. In this study, the loading conditions of an SSE were applied to obtain a conservative result. Figure 4 shows the results of the earthquake-proof analysis taking an earthquake into consideration. A maximum stress of 25.3kg$_f$/mm^2 was generated at the center of the ball, similar to the figure obtained when the earthquake was not considered.

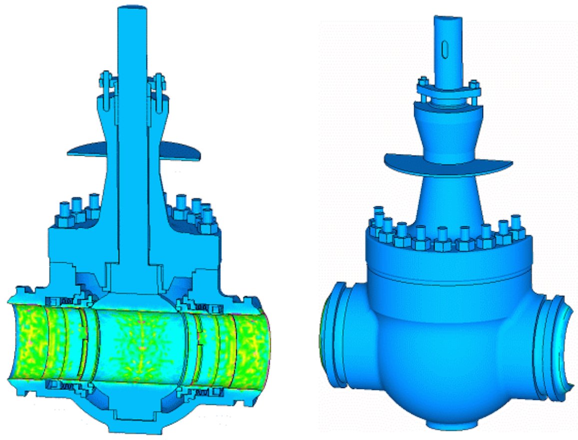

Figure 4 Results of the earthquake-proof analysis

Table 1 Seismic load condition for OBE and SSE

OBE	Vertical	±0.7g (dead weight : 1.0g)
	Horizontal	±1.0g
SSE	Vertical	±1.0g (dead weight : 1.0g)
	Horizontal	±1.5g

2.4. Flow Analysis

The flow analysis on the ball valve was carried out using FLUENT, which is a commercial CFD code with a model that includes 5 times the diameter to the upstream and 10 times the diameter to the downstream. Figure 5 shows the grid system for the numerical analysis. The grid system - a hybrid grid system - was a combination of arranged and non-arranged grids. The grids were allocated densely on the boundary wall to obtain a more precise prediction. The grid's density was made to be higher at the inlet and outlet to analyze eddy flow. The grid had 600,000 nodes for numerical analysis.

The entrance conditions of the analysis model, which were the pressure inlet conditions, were 168kg/cm^2 and 80kg/cm^2, and the exit condition was the atmospheric pressure. The internal temperature was set at -196℃, which is the temperature of LNG. The fluid was assumed to be methane, which accounts for approximately 90% of the composition of LNG (Alaskan). Table 2 presents the physical properties of methane.

Figure 5 Computational grid system of Ball valve

Table 2 Properties of Methane

Properties	Ball Valve	Properties	Ball Valve
Molecular weight	16	Critical pressure	45.8atm
Specific gravity	0.55	Explosion range	5~15% (in Air)
Boiling point	-161.5℃	Ignition point	550℃
Critical temperature	-82.1℃	Melting point	-182.4℃

Figure 6 shows the path lines and velocity distribution vector of the fluid particles. The path lines show relatively uniform velocity distribution, which can be identified by the velocity vector. It can be seen that the speed of the current accelerates after the valve. Figure 7 shows the velocity distribution at a cross-section when in a fully open state. It can be seen that the flow profiles of the cross-sections are similar, and faster, at the center. Figure 8 shows the velocity distribution at the distances of 100cm, 250cm, and 500cm from the valve outlet. On the graph, it can be seen that the velocity is distributed uniformly before and after the valve, and increases as the LNG flows downwards. The velocity profile takes the form of a parabola, which is the typical representation of velocity distribution.

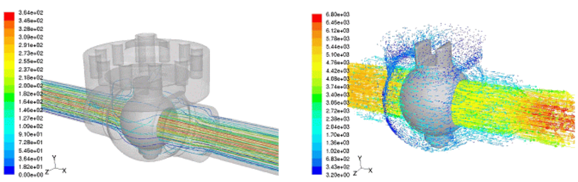

(a) Path lines (b) Velocity

Figure 6 Path lines & Velocity of fully opened state

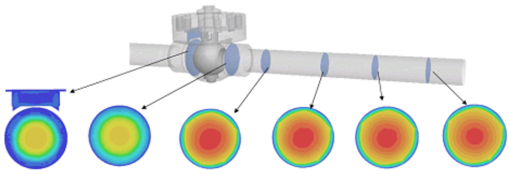

Figure 7 Velocity distributions of cross sectional area

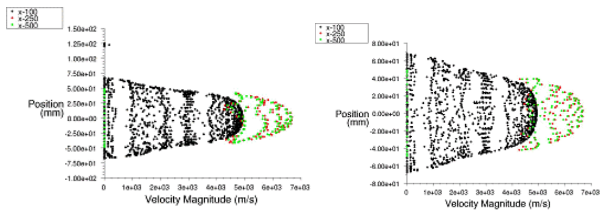

(a) y-direction (b) z-direction

Figure 8 Velocity distribution graphs

3. Design and Fabrication of Parts

3.1. Body Design

In general, the most important factor to be considered in designing a cryogenic valve is to obtain sufficient strength against internal pressure. This is the most important factor in the design of the pressure vessels; a valve body cannot be designed without careful consideration of the structural strength. In this study, the structural strength, contraction according to the valve configuration, and heat transfer with the extremely low temperature of LNG were analyzed and designed by simulation of the valve body.

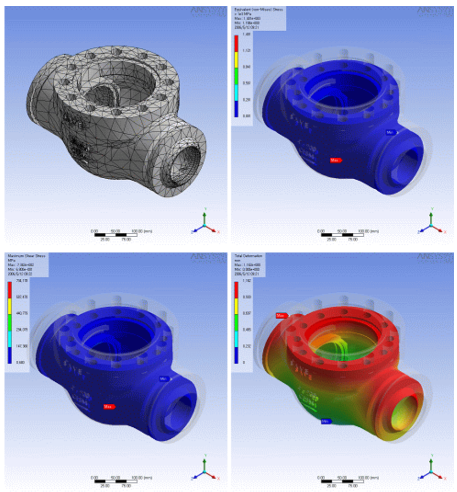

Figure 9 Analysis of Body

3.2. Design and Fabrication of the Seat

In top-entry type cryogenic ball valves, the most important component is the seal, which is very difficult to design and manufacture. Figure 10 shows the structure of a U-cup seal seat, whose test results at very low temperature are presented in Table 3. As the shrinkage rates of a U=cup seal and graphite are lower than that of stainless steel, leakage occurs at the seal at temperatures lower than -196℃. It can be seen that, although leakage under such conditions meets the BS 6364 Standard, it does not meet the specifications of the Korea Gas Corporation and LNG container vessels. Therefore, the seal was modified into a bellows-shape, which is shown in Figure 11.

Internal leakage through the seat was tested after assembling the seat, and there was almost no leakage through the bellows-type seat.

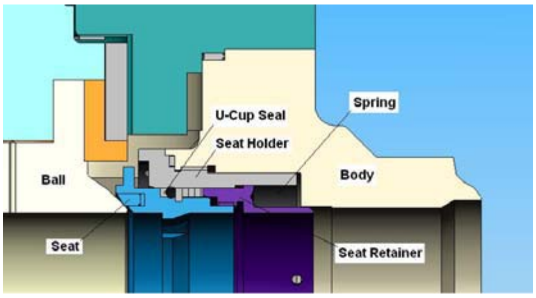

Figure 10 Structure of U-Cup Seal Seat

Table 3 Result of Leakage test

Valve Size	Test Result	Standard		
		BS 6364	KOGAS	LNG vessel
2"	200 cc/min	300 cc/min	10 cc/min	20 cc/min
4"	580 cc/min	600 cc/min	20 cc/min	40 cc/min

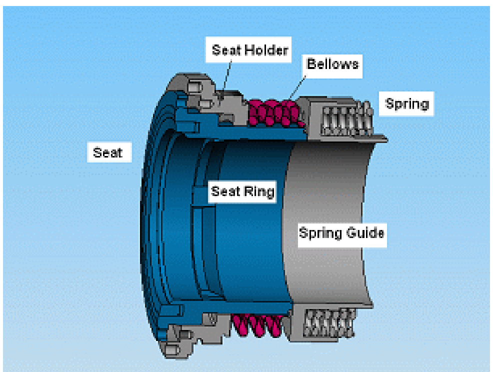

Figure 11 Structure of Bellows Seal Type Seat

3.3. Bonnet Design

A bonnet positioned at the central axis of a valve connects the handle and ball. If icing occurs at the packing, which is located in the upper part, due to low temperature in the lower part, then the LNG may leak. Therefore, a method of preventing icing and a design which can insulate the packing from low temperature in the valve are required. In this study, a heat insulating plate was used and the bonnet length was optimized through analysis and testing. Figure 12 shows the exterior configuration and temperature distribution of the bonnet. Figure 13 shows the measurement of heat transfer to the various parts of the bonnet.

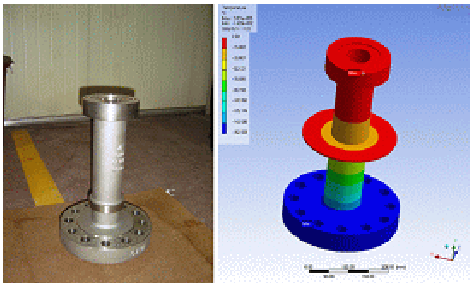

Figure 12 Temperature distributions of Bonnet

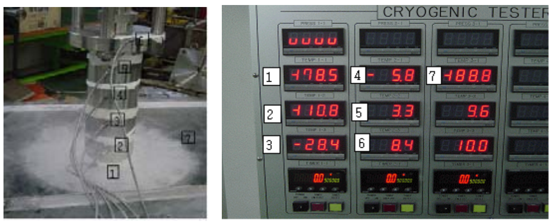

Figure 13 Measuring temperature distribution

3.4. Ball Design

Figure 14 shows the appearance and thermal deformation of the ball. It can be seen that the deformation caused by temperature variance has a constant distribution.

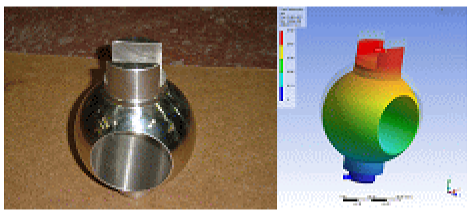

Figure 14 Thermal deformations of Ball

3.5. Spring Design

In a bellows-seal type seat, the pressure on surface of the bellows increases as the internal pressure of the valve increases, because the internal pressure is exerted on the effective area of the bellows. However, as the spring force of the bellows is weak at low pressure, a spring is required to press the bellows in order to prevent leakage from the seat during low pressure by maintaining the proper seating force. Table 4 presents the design data of the spring.

Table. 4 Design data of Spring

Item	Dia. (mm)	active coils (turns)	Spring Constant (kg_f/mm)	Free length (mm)	Length (mm)	Quantity (es)	Setting Force (kg_f)
Value	14.1	5	10.71	33	28	20	1,071

3.6. Fabrication of the Ball Valve

A high-pressure, cryogenic ball valve capable of ensuring zero-leakage was designed, as shown in Figure 15, after analysis the thermal stress, resistance against earthquake, and flow characteristics, and ensuring the optimal design of each part.

Figure 15 Cryogenic ball valve fabricated in this study

4. CONCLUSION

In order to examine the performance characteristics of the parts of high-pressure, cryogenic ball valves, numerical analyses of the strength and thermal shock were conducted and the seat structure was investigated and tested. The following conclusion was obtained.

1. According to the thermal stress analysis conducted at high pressure and very low temperature, a maximum stress of 23.9kg_f/mm^2 occurred at the center of the ball.
2. The resistance against earthquake was analyzed at a maximum acceleration of 2.0g in the vertical direction (z axis), including the self-weight, and 1.5g in the x and y axes, at high pressure and very low temperature, to obtain a maximum stress of 25.3kg_f/mm^2 at the center of the ball.
3. The flow characteristics of the ball valve were analyzed with inlet and outlet pressures of 168kg/cm^2 and 80kg/cm^2, respectively, to obtain the velocity distribution and eddy flow of LNG according to the valve position.
4. The design of the constituent parts of the ball valve, including the body, seat, bonnet, ball and spring, were optimized.
5. In this study, a high-pressure, cryogenic ball valve that can achieve zero leakage was designed.

ACKNOWLEDGEMENTS

This study is a part of the "Top Entry Type High-Pressure, Cryogenic Ball Valve Development Project," which is a parts and material development technology project sponsored by the Ministry of Commerce, Industry and Energy.

REFERENCES

1. Eleftherakis, John G. 1991, "Determining valve contaminant sensitivity effect using two contaminants", SAE TP 910960, pp459～464.
2. Thompson G, Askari, A.R. 1986, "Air leak detection through ball plug valves by vibration monitoring", Noise & Vibration control worldwide, V17, pp140-143.
3. Rouss, Gino james Janna, William S. 2003, "Determination of discharge coefficient for ball valves with calibrated inserts", 2003 ASME Mechanical engineering congress, pp 1~10.
4. Merati, P., Macelt, M.J, 2001, "Flow investigate around a v-sector ball valve" , 2001 ASME Fluids engineering, vol.123, no.3, pp662~671.